Non-singular spherical harmonic expressions of geomagnetic vector and gradient tensor fields in the local north-oriented reference frame

By

Jinsong Du[1,2,3]
Chao Chen[1]
Vincent Lesur[2]
and
Linsong Wang[1,3]

[1]Hubei Subsurface Multi-scale Imaging Key Laboratory, Institute of Geophysics & Geomatics, China University of Geosciences, Wuhan 430074, China
[2]Helmholtz Centre Potsdam, GFZ German Research Centre for Geosciences, Telegrafenberg 14473, Germany
[3]State Key Laboratory of Geodesy and Earth's Dynamics, Chinese Academy of Sciences, Wuhan 430077, China

Corresponding author:
Jinsong Du
Institute of Geophysics and Geomatics
China University of Geosciences
388 Lumo Road, Hongshan District, Wuhan 430074, P. R. China
E-mail: jinsongdu@gmail.com.cn
Tel.: +86-027-6788 3635
Fax.: +86-027-6788 3251

Submitted to
Technical, Development and Evaluation papers
in
Geoscientific Model Development

Discussion Paper Received: 27 October 2014
Discussion Paper Accepted: 4 November 2014
Discussion Paper Published: 5 December 2014
Revised Paper for GMD Received: 5 May 2015

Non-singular spherical harmonic expressions of geomagnetic vector and gradient tensor fields in the local north-oriented reference frame

Jinsong Du[1,2,3], Chao Chen[1], Vincent Lesur[2], and Linsong Wang[1,3]

[1]Hubei Subsurface Multi-scale Imaging Key Laboratory, Institute of Geophysics & Geomatics, China University of Geosciences, Wuhan 430074, China. E-mail: jinsongdu.cug@gmail.com

[2]Helmholtz Centre Potsdam, GFZ German Research Centre for Geosciences, Telegrafenberg 14473, Germany

[3]State Key Laboratory of Geodesy and Earth's Dynamics, Chinese Academy of Sciences, Wuhan 430077, China

Abstract

General expressions of magnetic vector (MV) and magnetic gradient tensor (MGT) in terms of the first- and second-order derivatives of spherical harmonics at different degrees/orders, are relatively complicated and singular at the poles. In this paper, we derived alternative non-singular expressions for the MV, the MGT and also the third-order partial derivatives of the magnetic potential field in local north-oriented reference frame. Using our newly derived formulae, the magnetic potential, vector and gradient tensor fields and also the third-order partial derivatives of the magnetic potential field at an altitude of 300 km are calculated based on a global lithospheric magnetic field model GRIMM_L120 (version 0.0) with spherical harmonic degrees 16~90. The corresponding results at the poles are discussed and the validity of the derived formulas is verified using the Laplace equation of the magnetic potential field.

1 Introduction

Compared to the magnetic vector and scalar measurements, magnetic gradients lead to more robust models of the lithospheric magnetic field. The ongoing *Swarm* mission of the European

Space Agency (ESA) provides measurements not only of the vector and scalar data but also an estimate of their east-west gradients (e.g. Olsen et al., 2004, 2015; Friis-Christensen et al., 2006). Kotsiaros and Olsen (2012, 2014) proposed to recover the lithospheric magnetic field through Magnetic Space Gradiometry in the same way that has been done for modeling the gravitational potential field from the satellite gravity gradient tensor measurements by the Gravity field and steady-state Ocean Circulation Explorer (GOCE). Purucker et al. (2005, 2007), Sabaka et al. (2015) and Kotsiaros et al. (2015) also reported efforts to model the lithospheric magnetic field using magnetic gradient information from the satellite constellation. Their results showed that by using gradients data, the modelled lithospheric magnetic anomaly field has enhanced shorter wavelength content and has a much higher quality compared to models built from vector field data. This is because the gradients data can remove the highly time-dependant contributions of the magnetosphere and ionosphere that are correlated between two side-by-side satellites.

The order-2 magnetic gradient tensor consists of spatial derivatives highlighting certain structures of the magnetic field (e.g. Schmidt and Clark, 2000, 2006). It can be used to detect the hidden and small-scale magnetized sources (e.g. Pedersen and Rasmussen, 1990; Harrison and Southam, 1991) and to investigate the orientation of the lineated magnetic anomalies (e.g. Blakely and Simpson, 1986). Quantitative magnetic interpretation methods such as the analytic signal, edge detection, spatial derivatives, Euler deconvolution, and transforms, all set in Cartesian coordinate system (e.g. Blakely, 1995; Purucker and Whaler, 2007; Taylor et al., 2014) also require calculating the higher-order derivatives of the magnetic anomaly field and need to be extended to regional and global scales to handle the curvature of the Earth and other planets. Ravat et al. (2002) and Ravat (2011) utilized the analytic signal method and the total gradient to interpret

48 the satellite-altitude magnetic anomaly data. Therefore, both the magnetic field modelling and also
49 the geological interpretations require the calculation for the partial derivatives of the magnetic
50 field, possibly at the poles for specific systems of coordinates. Spherical harmonic analysis,
51 established originally by Gauss (1839), is generally used to model the global magnetic internal
52 fields of the Earth and other terrestrial planets (e.g. Maus et al., 2008; Langlais et al., 2009;
53 Thébault et al., 2010, Finlay et al., 2010; Lesur et al., 2013, Sabaka et al., 2013; Olsen et al., 2014).
54 Series of spherical harmonic functions themselves made of Schmidt semi-normalized associated
55 Legendre functions (SSALFs) (e.g. Blakely, 1995; Langel and Hinze, 1998), are fitted by
56 least-squares to magnetic measurements, giving the spherical harmonic coefficients (i.e. the
57 Gaussian coefficients) defining the model. Kotsiaros and Olsen (2012, 2014) presented the MV
58 and the MGT using a spherical harmonic representation and, of course, their expressions are
59 singular as they approach the poles. Even if there are satellite data gaps around the poles, it is
60 advisable to use non-singular spherical harmonic expressions for the MV and the MGT in case
61 airborne or shipborne magnetic data are utilized (e.g. Golynsky et al., 2013; Maus, 2010). A
62 rotation of the coordinate system is always possible to avoid the polar singularity, but this solution
63 is very ineffective for large data sets.

64 In this paper, following Petrovskaya and Vershkov (2006) and Eshagh (2008, 2009) for the
65 gravitational gradient tensor in the local north oriented, orbital reference and geocentric spherical
66 frames, the non-singular expressions in terms of spherical harmonics for the MV, the MGT and the
67 third-order derivatives of the magnetic potential field in the specially defined local-north-oriented
68 reference frame (LNORF) are presented. In the next section, the traditional expressions of the MV
69 and the MGT are first stated, then some necessary propositions are proved and at last new

70 non-singular expressions are derived. In section 3, the new formulae are tested using the global
71 lithospheric magnetic field model GRIMM_L120 (version 0.0) (Lesur et al., 2013) and compared
72 with the results by traditional formulae. Finally, some conclusions are drawn and further
73 applications are also discussed.
74
75 **2 Methodology**
76 In this section, the traditional expressions of MV and MGT are presented, and their numerical
77 problems are stated. Then based on some necessary mathematical derivations, new expressions are
78 given.
79 **2.1 Traditional expressions**
80 The scalar potential V of the Earth′s magnetic field in a source-free region can be expanded in the
81 truncated series of spherical harmonics at the point $P(r, \theta, \varphi)$ with the geocentric distance r,
82 co-latitude θ and longitude φ (e.g. Backus et al., 1996):
83 $$V(r,\theta,\varphi) = a\sum_{l=1}^{L}\sum_{m=0}^{l}\left(\frac{a}{r}\right)^{l+1}\left(g_l^m \cos m\varphi + h_l^m \sin m\varphi\right)\widetilde{P}_l^m\left(\cos\theta\right), \quad (1)$$
84 where a=6371.2 km is the radius of the Earth's magnetic reference sphere; $\widetilde{P}_l^m\left(\cos\theta\right)$ (or $\widetilde{P}_l^m$
85 for simplification) is the SSALF of degree l and order m; L is the maximum spherical harmonic
86 degree; g_l^m and h_l^m are the geomagnetic harmonic coefficients describing internal sources of
87 the Earth.
88 If considered in the LNORF $\{\mathbf{x},\mathbf{y},\mathbf{z}\}$ (e.g. Olsen et al., 2010), where **z**-axis points downward in
89 geocentric radial direction, **x**-axis points to the north, and **y**-axis towards the east (that is, a
90 right-handed system). At the poles, we define that the **x**-axis points to the meridian of 180° E (or

180° W) at north pole and of 0° at south pole, which will be discussed in section 3. Therefore, the three components of the MV can be expressed as:

$$B_x(r,\theta,\varphi) = -\frac{1}{r}\frac{\partial}{\partial(-\theta)}V(r,\theta,\varphi)$$
$$= \sum_{l=1}^{L}\sum_{m=0}^{l}\left(\frac{a}{r}\right)^{l+2}\left(g_l^m\cos m\varphi + h_l^m\sin m\varphi\right)\left[\frac{\partial}{\partial\theta}\widetilde{P}_l^m(\cos\theta)\right], \quad (2a)$$

$$B_y(r,\theta,\varphi) = -\frac{1}{r\sin\theta}\frac{\partial}{\partial\varphi}V(r,\theta,\varphi)$$
$$= \sum_{l=1}^{L}\sum_{m=0}^{l}\left(\frac{a}{r}\right)^{l+2} m\left(g_l^m\sin m\varphi - h_l^m\cos m\varphi\right)\left[\frac{1}{\sin\theta}\widetilde{P}_l^m(\cos\theta)\right], \quad (2b)$$

$$B_z(r,\theta,\varphi) = -\frac{\partial}{\partial(-r)}V(r,\theta,\varphi)$$
$$= -\sum_{l=1}^{L}\sum_{m=0}^{l}(l+1)\left(\frac{a}{r}\right)^{l+2}\left(g_l^m\cos m\varphi + h_l^m\sin m\varphi\right)\widetilde{P}_l^m(\cos\theta). \quad (2c)$$

The MGT can be written as (e.g. Kotsiaros and Olsen, 2012)

$$\nabla\mathbf{B} = \begin{pmatrix} B_{xx} & B_{xy} & B_{xz} \\ B_{yx} & B_{yy} & B_{yz} \\ B_{zx} & B_{zy} & B_{zz} \end{pmatrix} = \begin{pmatrix} \partial B_x/\partial x & \partial B_x/\partial y & \partial B_x/\partial z \\ \partial B_y/\partial x & \partial B_y/\partial y & \partial B_y/\partial z \\ \partial B_z/\partial x & \partial B_z/\partial y & \partial B_z/\partial z \end{pmatrix}, \quad (3)$$

where nine elements are expressed respectively as:

$$B_{xx} = \frac{1}{a}\sum_{l=1}^{L}\sum_{m=0}^{l}\left(\frac{a}{r}\right)^{l+3}\left(g_l^m\cos m\varphi + h_l^m\sin m\varphi\right)$$
$$\times\left[-\frac{\partial^2}{\partial\theta^2}\widetilde{P}_l^m(\cos\theta) + (l+1)\widetilde{P}_l^m(\cos\theta)\right], \quad (4a)$$

$$B_{xy} = B_{yx} = \frac{1}{a}\sum_{l=1}^{L}\sum_{m=0}^{l}\left(\frac{a}{r}\right)^{l+3} m\left(g_l^m\sin m\varphi - h_l^m\cos m\varphi\right)$$
$$\times\left[-\frac{1}{\sin\theta}\frac{\partial}{\partial\theta}\widetilde{P}_l^m(\cos\theta) + \frac{\cos\theta}{\sin^2\theta}\widetilde{P}_l^m(\cos\theta)\right], \quad (4b)$$

$$B_{xz} = B_{zx} = \frac{1}{a}\sum_{l=1}^{L}\sum_{m=0}^{l}\left(\frac{a}{r}\right)^{l+3}(l+2)\left(g_l^m\cos m\varphi + h_l^m\sin m\varphi\right)\left[\frac{\partial}{\partial\theta}\widetilde{P}_l^m(\cos\theta)\right], \quad (4c)$$

$$B_{yy}=\frac{1}{a}\sum_{l=1}^{L}\sum_{m=0}^{l}\left(\frac{a}{r}\right)^{l+3}\left(g_l^m\cos m\varphi+h_l^m\sin m\varphi\right)$$
$$\times\left[(l+1)\widetilde{P}_l^m(\cos\theta)+\frac{m^2}{\sin^2\theta}\widetilde{P}_l^m(\cos\theta)-\frac{\cos\theta}{\sin\theta}\frac{\partial}{\partial\theta}\widetilde{P}_l^m(\cos\theta)\right], \quad (4d)$$

$$B_{yz}=B_{zy}=\frac{1}{a}\sum_{l=1}^{L}\sum_{m=0}^{l}\left(\frac{a}{r}\right)^{l+3}(l+2)m\left(g_l^m\sin m\varphi-h_l^m\cos m\varphi\right)\left[\frac{1}{\sin\theta}\widetilde{P}_l^m(\cos\theta)\right], \quad (4e)$$

$$B_{zz}=-\frac{1}{a}\sum_{l=1}^{L}\sum_{m=0}^{l}\left(\frac{a}{r}\right)^{l+3}(l+1)(l+2)\left(g_l^m\cos m\varphi+h_l^m\sin m\varphi\right)\widetilde{P}_l^m(\cos\theta) \quad . \quad (4f)$$

The expressions for V, B_z and B_{zz} can be calculated stably even for very high spherical harmonic degrees and orders by using the Holmes and Featherstone (2002a) scheme. However, there exist the singular terms of $1/\sin\theta$ and $1/\sin^2\theta$ in Eq. (2b), Eq. (4b), Eq. (4d) and Eq. (4e) when the computing point approaches to the poles. Besides, some expressions contain the terms of first- and second-order derivatives of SSALFs, such as Eq. (2a) and Eq. (4a) ~ (4d). Nevertheless, the derivatives up to second-order for very high degree and orders of SSALFs can be recursively calculated by the Horner algorithm (Holmes and Featherstone, 2002b). These algorithms are relatively complicated and thus we want to use alternative expressions to avoid the singular terms and also the partial derivatives of SSALFs. It should be stated that our work differs from those presented by Petrovskaya and Vershkov (2006) and Eshagh (2009) in the LNORF and also the associated Legendre functions (ALFs). Nonetheless, the following mathematical derivations are carried out based on their studies in gravity field.

2.2 Mathematical derivations

To deal with the singular terms and first- and second-order derivatives of the SSALFs, some useful mathematical derivations are introduced and proved in the following.

1 - Derivation of $\partial\widetilde{P}_l^m/\partial\theta$:

Based on Eq. (Z.1.44) in Ilk (1983)

$$\partial P_l^m / \partial\theta = 0.5\left[(l+m)(l-m+1)P_l^{m-1} - P_l^{m+1}\right], \tag{5}$$

and the relation between the ALFs and the SSALFs as

$$\widetilde{P}_l^m = \sqrt{C_m (l-m)!/(l+m)!}\,P_l^m, \tag{6}$$

thus the first-order derivative of the SSALFs can be deduced as:

$$\partial \widetilde{P}_l^m / \partial\theta = a_{l,m}\widetilde{P}_l^{m-1} + b_{l,m}\widetilde{P}_l^{m+1}, \tag{7a}$$

$$a_{l,m} = 0.5\sqrt{l+m}\sqrt{l-m+1}\sqrt{C_m / C_{m-1}}, \tag{7b}$$

$$b_{l,m} = -0.5\sqrt{l+m+1}\sqrt{l-m}\sqrt{C_m / C_{m+1}}, \tag{7c}$$

where $C_m = 2 - \delta_{m,0} = \begin{cases} 1, m = 0 \\ 2, m \neq 0 \end{cases}$ and δ is the Kronecker delta.

2 - Derivation of $\partial^2 \widetilde{P}_l^m / \partial\theta^2$:

According to Eq. (23) in Eshagh (2008) as

$$\begin{aligned} \partial^2 P_l^m / \partial\theta^2 = {} & 0.25(l+m)(l-m+1)(l+m-1)(l-m+2)P_l^{m-2} \\ & - 0.25\left[(l+m)(l-m+1) + (l-m)(l+m+1)\right]P_l^m \\ & + 0.25P_l^{m+2} \end{aligned}, \tag{8}$$

the second-order derivative of the SSALFs can be written as:

$$\partial^2 \widetilde{P}_l^m / \partial\theta^2 = c_{l,m}\widetilde{P}_l^{m-2} + d_{l,m}\widetilde{P}_l^m + e_{l,m}\widetilde{P}_l^{m+2}, \tag{9a}$$

$$c_{l,m} = 0.25\sqrt{l+m}\sqrt{l+m-1}\sqrt{l-m+2}\sqrt{l-m+1}\sqrt{C_m / C_{m-2}}, \tag{9b}$$

$$d_{l,m} = -0.25\left[(l+m)(l-m+1) + (l-m)(l+m+1)\right], \tag{9c}$$

$$e_{l,m} = 0.25\sqrt{l+m+2}\sqrt{l+m+1}\sqrt{l-m}\sqrt{l-m-1}\sqrt{C_m / C_{m+2}}. \tag{9d}$$

3 - Derivation of $\widetilde{P}_l^m / \sin\theta$:

Using Eq. (Z.1.42) in Ilk (1983)

$$P_l^m / \sin\theta = 0.5\left[(l+m)(l+m-1)P_{l-1}^{m-1} + P_{l-1}^{m+1}\right]/m, \; m \geq 1, \tag{10}$$

and Eq. (6), we can obtain that

142 $$\widetilde{P}_l^m / \sin\theta = f_{l,m}\widetilde{P}_{l-1}^{m-1} + g_{l,m}\widetilde{P}_{l-1}^{m+1} \quad , m \geq 1 \,, \tag{11a}$$

143 $$f_{l,m} = 0.5\sqrt{l+m}\sqrt{l+m-1}\sqrt{C_m / C_{m-1}} / m \quad , m \geq 1 \,, \tag{11b}$$

144 $$g_{l,m} = 0.5\sqrt{l-m}\sqrt{l-m-1}\sqrt{C_m / C_{m+1}} / m \quad , m \geq 1 \,. \tag{11c}$$

145 4 - Derivation of $\widetilde{P}_l^m / \sin^2\theta$:

146 Employing Eq. (31) in Eshagh (2008) as

$$\begin{aligned} P_l^m / \sin^2\theta = \{&(l+m)(l+m-1)(l-m+1)(l-m+2)/(m-1)P_l^{m-2} \\ &+ [(l+m)(l+m-1)/(m-1) + (l-m)(l-m-1)/(m+1)]P_l^m \\ &+ 1/(m+1)P_l^{m+2}\}/(4m) \end{aligned} \quad , m \geq 2 \,, \tag{12}$$

147

148 and Eq. (6), we have

149 $$\widetilde{P}_l^m / \sin^2\theta = h_{l,m}\widetilde{P}_l^{m-2} + k_{l,m}\widetilde{P}_l^m + n_{l,m}\widetilde{P}_l^{m+2} \quad , m \geq 2 \,, \tag{13a}$$

150 $$h_{l,m} = 0.25\sqrt{l+m}\sqrt{l+m-1}\sqrt{l-m+1}\sqrt{l-m+2}\sqrt{C_m / C_{m-2}} / [m(m-1)] \quad , m \geq 2 \,, \tag{13b}$$

151 $$k_{l,m} = 0.25[(l+m)(l+m-1)/(m-1) + (l-m)(l-m-1)/(m+1)] / m \quad , m \geq 2 \,, \tag{13c}$$

152 $$n_{l,m} = 0.25\sqrt{l-m}\sqrt{l-m-1}\sqrt{l+m+2}\sqrt{l+m+1}\sqrt{C_m / C_{m+2}} / [m(m+1)] \quad , m \geq 1 \,. \tag{13d}$$

153 5 - Derivation of $\partial\widetilde{P}_l^m / (\sin\theta\partial\theta)$:

154 Using Eq. (36) in Eshagh (2008) as

$$\begin{aligned} \partial P_l^m / (\sin\theta\partial\theta) = 0.25\{&(l+m)(l+m-1)(l+m-2)(l-m+1)/(m-1)P_{l-1}^{m-2} \\ &+ [(l+m)(l-m+1)/(m-1) - (l+m+1)(l+m)/(m+1)]P_{l-1}^m \\ &- 1/(m+1)P_{l-1}^{m+2}\} \end{aligned} \quad , m \geq 2 \,, \tag{14}$$

155

156 and Eq. (6), we can derive

157 $$\partial\widetilde{P}_l^m / (\sin\theta\partial\theta) = o_{l,m}\widetilde{P}_{l-1}^{m-2} + q_{l,m}\widetilde{P}_{l-1}^m + x_{l,m}\widetilde{P}_{l-1}^{m+2} \quad , m \geq 2 \,, \tag{15a}$$

158 $$o_{l,m} = 0.25\sqrt{l+m}\sqrt{l+m-1}\sqrt{l+m-2}\sqrt{l-m+1}\sqrt{C_m / C_{m-2}} / (m-1) \quad , m \geq 2 \,, \tag{15b}$$

159 $$q_{l,m} = 0.25\sqrt{l-m}\sqrt{l+m}[(l-m+1)/(m-1) - (l+m+1)/(m+1)] \quad , m \geq 2 \,, \tag{15c}$$

160 $$x_{l,m} = -0.25\sqrt{(l+m+1)}\sqrt{l-m}\sqrt{l-m-1}\sqrt{l-m-2}\sqrt{C_m / C_{m+2}} / (m+1) \,. \tag{15d}$$

161 6 - Derivation of $\partial\widetilde{P}_l^m / (\sin\theta\partial\theta) - \widetilde{P}_l^m \cos\theta / \sin^2\theta$:

According to Petrovskaya and Vershkov (2006) and Eshagh (2009), we can write

$$\begin{aligned}&\partial P_l^m/\left(\sin\theta\partial\theta\right)-P_l^m\cos\theta/\sin^2\theta\\&=0.5\left[\left(m-1\right)\left(l+m\right)\left(l-m+1\right)P_l^{m-1}/\sin\theta-\left(m+1\right)P_l^{m+1}/\sin\theta\right]/m\end{aligned},\ m\geq 1, \tag{16}$$

and using Eq. (36) in Eshagh (2008), we can obtain

$$P_l^{m-1}/\sin\theta=0.5\left[\left(l-m+2\right)\left(l-m+3\right)P_{l+1}^{m-2}+P_{l+1}^m\right]/\left(m-1\right),\ m\geq 2, \tag{17a}$$

$$P_l^{m+1}/\sin\theta=0.5\left[\left(l-m\right)\left(l-m+1\right)P_{l+1}^m+P_{l+1}^{m+2}\right]/\left(m+1\right). \tag{17b}$$

Substituting Eq. (17) into the right hand side of Eq. (16) and after simplification, we can derive

$$\begin{aligned}&\partial P_l^m/\left(\sin\theta\partial\theta\right)-P_l^m\cos\theta/\sin^2\theta\\&=0.25\left[\left(l+m\right)\left(l-m+1\right)\left(l-m+2\right)\left(l-m+3\right)P_{l+1}^{m-2}\right.\\&\left.+2m\left(l-m+1\right)P_{l+1}^m-P_{l+1}^{m+2}\right]/m\end{aligned},\ m\geq 1. \tag{18}$$

And combing Eq. (6), we obtain that

$$\begin{aligned}&\partial\widetilde{P}_l^m/\left(\sin\theta\partial\theta\right)-\widetilde{P}_l^m\cos\theta/\sin^2\theta\\&=0.25\left[\sqrt{l+m}\sqrt{l-m+1}\sqrt{l-m+2}\sqrt{l-m+3}\sqrt{C_m/C_{m-2}}\widetilde{P}_{l+1}^{m-2}\right.\\&+2m\sqrt{l-m+1}\sqrt{l+m+1}\widetilde{P}_{l+1}^m\\&\left.-\sqrt{l+m+1}\sqrt{l+m+2}\sqrt{l+m+3}\sqrt{l-m}\sqrt{C_m/C_{m+2}}\widetilde{P}_{l+1}^{m+2}\right]/m\end{aligned},\ m\geq 1. \tag{19}$$

7 - Derivation of $\left[\left(l+1\right)\sin^2\theta\widetilde{P}_l^m+m^2\widetilde{P}_l^m-\sin\theta\cos\theta\partial\widetilde{P}_l^m/\partial\theta\right]/\sin^2\theta$:

Based on Lemma 3 in Eshagh (2009) as

$$\sin\theta\cos\theta\partial P_l^m/\partial\theta=mP_l^m+\left(l+1\right)\sin^2\theta P_l^m-\sin\theta P_{l+1}^{m+1}, \tag{20}$$

we can derive

$$\begin{aligned}&\left[\left(l+1\right)\sin^2\theta P_l^m+m^2P_l^m-\sin\theta\cos\theta\partial P_l^m/\partial\theta\right]/\sin^2\theta\\&=m\left(m-1\right)P_l^m/\sin^2\theta+P_{l+1}^{m+1}/\sin\theta\end{aligned}. \tag{21}$$

According to Eq. (10), we can write

$$P_{l+1}^{m+1}/\sin\theta=0.5\left[\left(l+m+2\right)\left(l+m+1\right)P_l^m+P_l^{m+2}\right]/\left(m+1\right). \tag{22}$$

Inserting Eq. (12) and Eq. (22) into Eq. (21), and after some simplifications, we obtain that

$$
\begin{aligned}
&\left[(l+1)\sin^2\theta P_l^m + m^2 P_l^m - \sin\theta\cos\theta \partial P_l^m/\partial\theta\right]/\sin^2\theta \\
&= 0.25(l+m)(l+m-1)(l-m+1)(l-m+2)P_l^{m-2} \\
&+ 0.25\left[(l+m)(l+m-1)+(l-m)(l-m-1)(m-1)/(m+1)\right. \\
&\left.+ 2(l+m+2)(l+m+1)/(m+1)\right]P_l^m + 0.25P_l^{m+2}
\end{aligned}
\tag{23}
$$

And combing with Eq. (6), we can derive

$$
\begin{aligned}
&\left[(l+1)\sin^2\theta \widetilde{P}_l^m + m^2 \widetilde{P}_l^m - \sin\theta\cos\theta \partial \widetilde{P}_l^m/\partial\theta\right]/\sin^2\theta \\
&= 0.25\sqrt{l+m}\sqrt{l+m-1}\sqrt{l-m+1}\sqrt{l-m+2}\sqrt{C_m/C_{m-2}}\widetilde{P}_l^{m-2} \\
&+ 0.25\left[(l+m)(l+m-1)+(l-m)(l-m-1)(m-1)/(m+1)\right. \\
&\left.+ 2(l+m+2)(l+m+1)/(m+1)\right]\widetilde{P}_l^m \\
&+ 0.25\sqrt{l+m+1}\sqrt{l+m+2}\sqrt{l-m}\sqrt{l-m-1}\sqrt{C_m/C_{m+2}}\widetilde{P}_l^{m+2}
\end{aligned}
\tag{24}
$$

2.3 New expressions

Inserting the corresponding mathematical derivations in the last section into Eq. (2) and Eq. (4) and after some simplifications, the new expressions for MV and MGT can be written as:

$$
B_x = \sum_{l=1}^{L}\sum_{m=0}^{l}\left(\frac{a}{r}\right)^{l+2}\left(g_l^m\cos m\varphi + h_l^m\sin m\varphi\right)\left(a_{l,m}^x\widetilde{P}_l^{m-1} + b_{l,m}^x\widetilde{P}_l^{m+1}\right), \tag{25a}
$$

$$
B_y = \sum_{l=1}^{L}\sum_{m=0}^{l}\left(\frac{a}{r}\right)^{l+2}\left(g_l^m\sin m\varphi - h_l^m\cos m\varphi\right)\left(a_{l,m}^y\widetilde{P}_{l-1}^{m-1} + b_{l,m}^y\widetilde{P}_{l-1}^{m+1}\right), \tag{25b}
$$

$$
B_z = \sum_{l=1}^{L}\sum_{m=0}^{l}\left(\frac{a}{r}\right)^{l+2}\left(g_l^m\cos m\varphi + h_l^m\sin m\varphi\right)\left(a_{l,m}^z\widetilde{P}_l^m\right), \tag{25c}
$$

$$
B_{xx} = \frac{1}{a}\sum_{l=1}^{L}\sum_{m=0}^{l}\left(\frac{a}{r}\right)^{l+3}\left(g_l^m\cos m\varphi + h_l^m\sin m\varphi\right)\left(a_{l,m}^{xx}\widetilde{P}_l^{m-2} + b_{l,m}^{xx}\widetilde{P}_l^m + c_{l,m}^{xx}\widetilde{P}_l^{m+2}\right), \tag{26a}
$$

$$
B_{xy} = \frac{1}{a}\sum_{l=1}^{L}\sum_{m=0}^{l}\left(\frac{a}{r}\right)^{l+3}\left(g_l^m\sin m\varphi - h_l^m\cos m\varphi\right)\left(a_{l,m}^{xy}\widetilde{P}_{l+1}^{m-2} + b_{l,m}^{xy}\widetilde{P}_{l+1}^m + c_{l,m}^{xy}\widetilde{P}_{l+1}^{m+2}\right), \tag{26b}
$$

$$
B_{xz} = \frac{1}{a}\sum_{l=1}^{L}\sum_{m=0}^{l}\left(\frac{a}{r}\right)^{l+3}\left(g_l^m\cos m\varphi + h_l^m\sin m\varphi\right)\left(a_{l,m}^{xz}\widetilde{P}_l^{m-1} + b_{l,m}^{xz}\widetilde{P}_l^{m+1}\right), \tag{26c}
$$

$$
B_{yy} = \frac{1}{a}\sum_{l=1}^{L}\sum_{m=0}^{l}\left(\frac{a}{r}\right)^{l+3}\left(g_l^m\cos m\varphi + h_l^m\sin m\varphi\right)\left(a_{l,m}^{yy}\widetilde{P}_l^{m-2} + b_{l,m}^{yy}\widetilde{P}_l^m + c_{l,m}^{yy}\widetilde{P}_l^{m+2}\right), \tag{26d}
$$

$$B_{yz}=\frac{1}{a}\sum_{l=1}^{L}\sum_{m=0}^{l}\left(\frac{a}{r}\right)^{l+3}\left(g_l^m\sin m\varphi-h_l^m\cos m\varphi\right)\left(a_{l,m}^{yz}\widetilde{P}_{l-1}^{m-1}+b_{l,m}^{yz}\widetilde{P}_{l-1}^{m+1}\right), \tag{26e}$$

$$B_{zz}=\frac{1}{a}\sum_{l=1}^{L}\sum_{m=0}^{l}\left(\frac{a}{r}\right)^{l+3}\left(g_l^m\cos m\lambda+h_l^m\sin m\varphi\right)a_{l,m}^{zz}\widetilde{P}_l^m. \tag{26f}$$

where the corresponding coefficients of the SSALFs are given as following:

$$\begin{cases}a_{l,m}^{x}=0.5\sqrt{l+m}\sqrt{l-m+1}\sqrt{C_m/C_{m-1}}\\ b_{l,m}^{x}=-0.5\sqrt{l+m+1}\sqrt{l-m}\sqrt{C_m/C_{m+1}}\end{cases}, \tag{27a}$$

$$\begin{cases}a_{l,m}^{y}=0.5\sqrt{l+m}\sqrt{l+m-1}\sqrt{C_m/C_{m-1}}\\ b_{l,m}^{y}=0.5\sqrt{l-m}\sqrt{l-m-1}\sqrt{C_m/C_{m+1}}\end{cases}, \tag{27b}$$

$$a_{l,m}^{z}=-(l+1), \tag{27c}$$

$$\begin{cases}a_{l,m}^{xx}=-0.25\sqrt{l+m}\sqrt{l+m-1}\sqrt{l-m+2}\sqrt{l-m+1}\sqrt{C_m/C_{m-2}}\\ b_{l,m}^{xx}=0.25\left[(l+m)(l-m+1)+(l-m)(l+m+1)\right]+(l+1)\\ c_{l,m}^{xx}=-0.25\sqrt{l+m+2}\sqrt{l+m+1}\sqrt{l-m}\sqrt{l-m-1}\sqrt{C_m/C_{m+2}}\end{cases}, \tag{27d}$$

$$\begin{cases}a_{l,m}^{xy}=-0.25\sqrt{l+m}\sqrt{l-m+1}\sqrt{l-m+2}\sqrt{l-m+3}\sqrt{C_m/C_{m-2}}\\ b_{l,m}^{xy}=-0.5m\sqrt{l-m+1}\sqrt{l+m+1}\\ c_{l,m}^{xy}=0.25\sqrt{l+m+1}\sqrt{l+m+2}\sqrt{l+m+3}\sqrt{l-m}\sqrt{C_m/C_{m+2}}\end{cases}, \tag{27e}$$

$$\begin{cases}a_{l,m}^{xz}=0.5(l+2)\sqrt{l+m}\sqrt{l-m+1}\sqrt{C_m/C_{m-1}}=(l+2)a_{l,m}^{x}\\ b_{l,m}^{xz}=-0.5(l+2)\sqrt{l+m+1}\sqrt{l-m}\sqrt{C_m/C_{m+1}}=(l+2)b_{l,m}^{x}\end{cases}, \tag{27f}$$

$$\begin{cases}a_{l,m}^{yy}=0.25\sqrt{l+m}\sqrt{l+m-1}\sqrt{l-m+1}\sqrt{l-m+2}\sqrt{C_m/C_{m-2}}\\ b_{l,m}^{yy}=0.25\left[(l+m)(l+m-1)+(l-m)(l-m-1)(m-1)/(m+1)\right.\\ \qquad\left.+2(l+m+2)(l+m+1)/(m+1)\right]\\ c_{l,m}^{yy}=0.25\sqrt{l+m+1}\sqrt{l+m+2}\sqrt{l-m}\sqrt{l-m-1}\sqrt{C_m/C_{m+2}}\end{cases}, \tag{27g}$$

$$\begin{cases}a_{l,m}^{yz}=0.5(l+2)\sqrt{l+m}\sqrt{l+m-1}\sqrt{C_m/C_{m-1}}=(l+2)a_{l,m}^{y}\\ b_{l,m}^{yz}=0.5(l+2)\sqrt{l-m}\sqrt{l-m-1}\sqrt{C_m/C_{m+1}}=(l+2)b_{l,m}^{y}\end{cases}, \tag{27h}$$

$$a_{l,m}^{zz}=-(l+1)(l+2)=(l+2)a_{l,m}^{z}. \tag{27i}$$

Furthermore, some other higher-order partial derivatives and their transforms are usually used to image geologic boundaries in magnetic prospecting, such as the higher-order enhanced analytic

signal (e.g. Hsu et al., 1996). Therefore, we also give the third-order partial derivatives of the magnetic potential field as:

$$B_{xxz}=\frac{\partial B_{xx}}{\partial z}=\frac{\partial^2 B_x}{\partial x\partial z}=\frac{\partial^2 B_x}{\partial z\partial x}$$

$$=\frac{1}{a^2}\sum_{l=1}^{L}\sum_{m=0}^{l}\left(\frac{a}{r}\right)^{l+4}\left(g_l^m\cos m\varphi+h_l^m\sin m\varphi\right)\left(a_{l,m}^{xxz}\widetilde{P}_l^{m-2}+b_{l,m}^{xxz}\widetilde{P}_l^{m}+c_{l,m}^{xxz}\widetilde{P}_l^{m+2}\right), \quad (28a)$$

$$B_{xyz}=\frac{\partial B_{xy}}{\partial z}=\frac{\partial B_{yx}}{\partial z}=\frac{\partial^2 B_x}{\partial y\partial z}=\frac{\partial^2 B_x}{\partial z\partial y}=\frac{\partial^2 B_y}{\partial x\partial z}=\frac{\partial^2 B_y}{\partial z\partial x}$$

$$=\frac{1}{a^2}\sum_{l=1}^{L}\sum_{m=0}^{l}\left(\frac{a}{r}\right)^{l+4}\left(g_l^m\sin m\varphi-h_l^m\cos m\varphi\right)\left(a_{l,m}^{xyz}\widetilde{P}_{l+1}^{m-2}+b_{l,m}^{xyz}\widetilde{P}_{l+1}^{m}+c_{l,m}^{xyz}\widetilde{P}_{l+1}^{m+2}\right), \quad (28b)$$

$$B_{xzz}=\frac{\partial B_{xz}}{\partial z}=\frac{\partial B_{zx}}{\partial z}=\frac{\partial^2 B_x}{\partial z^2}=\frac{\partial^2 B_z}{\partial x\partial z}=\frac{\partial^2 B_z}{\partial z\partial x}$$

$$=\frac{1}{a^2}\sum_{l=1}^{L}\sum_{m=0}^{l}\left(\frac{a}{r}\right)^{l+4}\left(g_l^m\cos m\varphi+h_l^m\sin m\varphi\right)\left(a_{l,m}^{xzz}\widetilde{P}_l^{m-1}+b_{l,m}^{xzz}\widetilde{P}_l^{m+1}\right), \quad (28c)$$

$$B_{yyz}=\frac{\partial B_{yy}}{\partial z}=\frac{\partial^2 B_y}{\partial y\partial z}=\frac{\partial^2 B_y}{\partial z\partial y}$$

$$=\frac{1}{a^2}\sum_{l=1}^{L}\sum_{m=0}^{l}\left(\frac{a}{r}\right)^{l+4}\left(g_l^m\cos m\varphi+h_l^m\sin m\varphi\right)\left(a_{l,m}^{yyz}\widetilde{P}_l^{m-2}+b_{l,m}^{yyz}\widetilde{P}_l^{m}+c_{l,m}^{yyz}\widetilde{P}_l^{m+2}\right), \quad (28d)$$

$$B_{yzz}=\frac{\partial B_{yz}}{\partial z}=\frac{\partial B_{zy}}{\partial z}=\frac{\partial^2 B_y}{\partial z^2}=\frac{\partial^2 B_z}{\partial y\partial z}=\frac{\partial^2 B_z}{\partial z\partial y}$$

$$=\frac{1}{a^2}\sum_{l=1}^{L}\sum_{m=0}^{l}\left(\frac{a}{r}\right)^{l+4}\left(g_l^m\sin m\lambda-h_l^m\cos m\lambda\right)\left(a_{l,m}^{yzz}\widetilde{P}_{l-1}^{m-1}+b_{l,m}^{yzz}\widetilde{P}_{l-1}^{m+1}\right), \quad (28e)$$

$$B_{zzz}=\frac{\partial^2 B_z}{\partial z^2}$$

$$=\frac{1}{a^2}\sum_{l=1}^{L}\sum_{m=0}^{l}\left(\frac{a}{r}\right)^{l+4}\left(g_l^m\cos m\varphi+h_l^m\sin m\varphi\right)a_{l,m}^{zzz}\widetilde{P}_l^m, \quad (28f)$$

where the corresponding coefficients of the SSALFs are presented as:

$$\begin{cases}a_{l,m}^{xxz}=(l+3)a_{l,m}^{xx}\\ b_{l,m}^{xxz}=(l+3)b_{l,m}^{xx}\\ c_{l,m}^{xxz}=(l+3)c_{l,m}^{xx}\end{cases}, \quad (29a)$$

$$\begin{cases} a_{l,m}^{xyz} = (l+3)a_{l,m}^{xy} \\ b_{l,m}^{xyz} = (l+3)b_{l,m}^{xy} \\ c_{l,m}^{xyz} = (l+3)c_{l,m}^{xy} \end{cases}, \tag{29b}$$

$$\begin{cases} a_{l,m}^{xzz} = 0.5(l+2)(l+3)\sqrt{l+m}\sqrt{l-m+1}\sqrt{C_m / C_{m-1}} \\ \quad = (l+2)(l+3)a_{l,m}^{x} = (l+3)a_{l,m}^{xz} \\ b_{l,m}^{xzz} = -0.5(l+2)(l+3)\sqrt{l+m+1}\sqrt{l-m}\sqrt{C_m / C_{m+1}} \\ \quad = (l+2)(l+3)b_{l,m}^{x} = (l+3)b_{l,m}^{xz} \end{cases}, \tag{29c}$$

$$\begin{cases} a_{l,m}^{yyz} = (l+3)a_{l,m}^{yy} \\ b_{l,m}^{yyz} = (l+3)b_{l,m}^{yy} \\ c_{l,m}^{yyz} = (l+3)c_{l,m}^{yy} \end{cases}, \tag{29d}$$

$$\begin{cases} a_{l,m}^{yzz} = 0.5(l+2)(l+3)\sqrt{l+m}\sqrt{l+m-1}\sqrt{C_m / C_{m-1}} \\ \quad = (l+2)(l+3)a_{l,m}^{y} = (l+3)a_{l,m}^{yz} \\ b_{l,m}^{yzz} = 0.5(l+2)(l+3)\sqrt{l-m}\sqrt{l-m-1}\sqrt{C_m / C_{m+1}} \\ \quad = (l+2)(l+3)b_{l,m}^{y} = (l+3)b_{l,m}^{yz} \end{cases}, \tag{29e}$$

$$a_{l,m}^{zzz} = -(l+1)(l+2)(l+3) = (l+3)a_{l,m}^{zz} = (l+2)(l+3)a_{l,m}^{z}. \tag{29f}$$

In this way, we avoid computing recursively the SSALFs with singular terms, their first- and second-order derivatives as in the traditional formulae. The cost is only to calculate two additional degrees and orders for the SSALFs at most. It should be mentioned that, in this study, we use the conventional form of SSALF that if $m < 0$, then $\widetilde{P}_l^m = (-1)^{|m|}\widetilde{P}_l^{|m|}$ and if $m > l$, then $\widetilde{P}_l^m = 0$.

3 Numerical investigation and discussion

We test the derived expressions and the numerical implementation in C/C++, by calculating the magnetic potential, vector and its gradients and also the third-order partial derivatives of the magnetic potential field on a grid with 0.125°×0.125° cell size at the altitude of 300 km relative to the Earth′s magnetic reference sphere using the lithospheric magnetic field model GRIMM_L120

231 (version 0.0) defined by Lesur et al. (2013). The magnetic potential, MV, MGT and the third-order
232 partial derivatives of the magnetic potential field in the two polar regions mapped by the
233 lithospheric field model with spherical harmonic degrees/orders 16~90 are shown in Fig. 1 and Fig.
234 2, respectively. The corresponding statistics around the north and south poles are, respectively,
235 presented in Table 1 and Table 2. A simple test is that the MGT meets the Laplace's equation of the
236 potential field, that is, the trace of the MGT should be equal to zero. Our numerical results show
237 that the amplitudes of $B_{xx}+B_{yy}+B_{zz}$ in the north and south polar regions are in the range of
238 $[-2.012\times10^{-15}$ pT/m : $+2.026\times10^{-15}$ pT/m] (1 Tesla = 10^3 mT=10^9 nT=10^{12} pT=10^{18} aT),
239 respectively. The relative error is almost equal the machine accuracy. Therefore, this feature
240 proves the validity of our derived formulae. In addition, as shown in Fig. 1 and Fig. 2, it is obvious
241 that the MGT and also the third-order partial derivatives of the magnetic potential field enhance
242 the lineation and contacts at the satellite altitude. It also reveals some small-scale anomalies,
243 which is very helpful for the further geological interpretation. A core field model with spherical
244 harmonic degrees/orders 1~15 is also used to test and the results not shown here indicate the
245 correctness of the formulae in the full range of the spherical harmonic degrees/orders, where the
246 computational stability of the Legendre function with ultrahigh-order is not considered.
247 Furthermore, the computed magnetic fields are smooth near the poles and don't have the
248 singularities but some components have the dependence on the direction of reference frame at the
249 poles. As shown in Fig. 3, the magnetic potential V, B_z, B_{zz} and B_{zzz} components at the poles are
250 independent of the direction of the $\mathbf{x}_P$ and $\mathbf{y}_P$ axes, while changing with the direction of the $\mathbf{x}_P$ and
251 $\mathbf{y}_P$ axes at the poles, the B_x, B_y, B_{xz}, B_{yz}, B_{xzz} and B_{yzz} components have a period of 360° and the B_{xx},
252 B_{xy}, B_{yy}, B_{xxz}, B_{xyz} and B_{yyz} components have a period of 180°. These variations can be accurately

described by a sine or cosine function relating to the horizontal rotation of the reference frame and the differences among these magnetic effects are magnitude, period and initial phase. Therefore, B_x, B_y, B_{xz}, B_{yz}, B_{xx}, B_{xy}, B_{yy}, B_{xzz}, B_{yzz} B_{xxz}, B_{xyz} and B_{yyz} components are not smooth at/cross the poles. Therefore, to determine the single value at the poles (Fig. 1 and Fig. 2) we specially define that the **x**-axis points to the meridian of 180° E (or 180° W) at north pole and of 0° at south pole, that is, the LNORF moving from Greenwich meridian to the poles.

Compared with the traditional formulae in section 2.1, there are two advantages of our derived formulae in section 2.3. On the one hand, the traditional derivatives up to second-order are removed in the new formulae; therefore, the relatively complicated method by the Horner′s recursive algorithm (Holmes and Featherstone, 2002b) can be avoided. On the other hand, the singular terms of $1/\sin\theta$ and $1/\sin^2\theta$ are removed in the new formulae; consequently, the scale factor of e.g. 10^{-280} (Holmes and Featherstone, 2002a,b) is not required when the computing point approaches to the poles and the magnetic fields at the poles can also be calculated in the defined reference frame. In fact, there are differences between the results by our expressions and those by the Horner′s recursive algorithm, for instance, if using the same model and the parameters as those in Fig. 1 and Fig. 2, the differences of the three components B_x, B_y and B_z are at a level of [-3×10^{-11} nT : $+3\times10^{-11}$ nT].

4 Conclusions

We develop in this paper the new expressions for the MV, the MGT and the third-order partial derivatives of the magnetic potential field in terms of spherical harmonics. The traditional expressions have complicated forms involving first- and second-order derivatives of the SSALFs

and are singular when approaching to the poles. Our newly derived formulae don't contain the first- and second-order derivatives of the SSALFs and remove the singularities at the poles.

However, our formulae are derived in the spherical LNORF with specific definition at the poles. For an application to the magnetic data of a satellite gradiometry mission, it is necessary to describe the MV and the MGT in the local orbital or other reference frame, where the new MV and MGT are the linear functions of the MV and the MGT in the LNORF with coefficients related to the satellite track azimuth (e.g. Petrovskaya and Vershkov, 2006) or other rotation angles. The other main purpose of this paper is in the future to contribute to the signal processing and the geophysical & geological interpretation of global lithospheric magnetic field model, especially near polar areas.

Supplementary software implementation is performed by the programming language C/C++. The source code and input data presented in this paper can be obtained by contacting the lead author via email.

Acknowledgements. This study is supported by International Cooperation Projection in Science and Technology (No.: 2010DFA24580), Hubei Subsurface Multi-scale Imaging Key Laboratory (Institute of Geophysics & Geomatics, China University of Geosciences, Wuhan) (Grant No.: SMIL-2015-06) and State Key Laboratory of Geodesy and Earth's Dynamics (Institute of Geodesy and Geophysics, CAS) (Grant No.: SKLGED2015-5-5-EZ). Jinsong Du is sponsored by the China Scholarship Council (CSC). We would like to thank Prof. Mehdi Eshagh and another anonymous reviewer for their constructive suggestion. All projected figures are drawn using the Generic Mapping Tools (GMT) (Wessel and Smith, 1991).

297

298 **Refferences**

299 Backus, G. E., Parker, R., and Constable, C.: Foundations of Geomagnetism, Cambridge
300 University Press, Cambridge, 1996.

301 Blakely, R. J. and Simpson, R. W.: Approximating edges of source bodies from magnetic or
302 gravity anomalies, Geophysics, 51, 1494–1498, 1986.

303 Blakely, R. G.: Potential Theory in Gravity and Magnetic Applications, Cambridge University
304 Press, New York, 1995.

305 Bird, P.: An updated digital model of plate boundaries, Geochem. Geophys. Geosyst., 4(3), 1027,
306 doi:10.1029/2001GC000252, 2003.

307 Eshagh, M.: Non-singular expressions for the vector and gradient tensor of gravitation in a
308 geocentric spherical frame, Computers & Geosciences, 34, 1762–1768, 2008.

309 Eshagh, M.: Alternative expressions for gravity gradients in local north-oriented frame and tensor
310 spherical harmonics, Acta Geophysica, 58(2), 215–243, 2009.

311 Finlay, C. C., Maus, S., Beggan, C. D., Bondar, T. N., Chambodut, A., Chernova, T. A., Chulliat,
312 A., Golovkov, V. P., Hamilton, B., Hamoudi, M., Holme, R., Hulot, G., Kuang, W., Langlais, B.,
313 Lesur, V., Lowes, F. J., Lühr, H., Macmillan, S., Mandea, M., McLean, S., Manoj, C., Menvielle,
314 M., Michaelis, I., Olsen, N., Rauberg, J., Rother, M., Sabaka, T. J., Tangborn, A.,
315 Tøffner-Clausen, L., Thébault, E., Thomson, A. W. P., Wardinski, I., Wei, Z., and Zvereva, T. I.:
316 International Geomagnetic Reference Field: the eleventh generation, Geophys. J. Int., 183(3),
317 1216–1230, 2010.

318 Friis-Christensen, E., Lühr, H., and Hulot, G.: Swarm: A constellation to study the Earth's
319 magnetic field, Earth Planets Space, 58, 351–358, 2006.

320 Gauss, C. F.: Allgemeine Theorie des Erdmagnetismus, in: Resultate aus den Beobachtungen des
321 magnetischen vereins im Jahre 1838, edited by: Gauss, C. F. and Weber, W. (Leipzig, 1839),
322 1–57, 1838.

323 Golynsky, A., Bell, R., Blankenship, D., Damaske, D., Ferraccioli, F., Finn, C., Golynsky, D.,

Ivanov, S., Jokat, W., Masolov, V., Riedel, S., von Frese, R., Young, D., and ADMAP Working Group: Air and shipborne magnetic surveys of the Antarctic into the 21st century, Tectonophysics, 585, 3–12, 2013.

Harrison, C. and Southam, J.: Magnetic field gradients and their uses in the study of the Earth's magnetic field, J. Geomagn. Geoelectr., 43, 485–599, 1991.

Holmes, S. A. and Featherstone, W. E.: A unified approach to the Clenshaw summation and the recursive computation of very high degree and order normalized associated Legendre functions, J. Geod., 76, 279–299, 2002a.

Holmes, S. A. and Featherstone, W. E.: SHORT NOTES: extending simplified high-degree synthesis methods to second latitudinal derivatives of geopotential, J. Geod., 76, 447–450, 2002b.

Hsu, S. K., Sibuet, J. C., and Shyu, C. T.: High-resolution detection of geologic boundaries from potential-field anomalies: An enhanced analytic signal technique, Geophysics, 61(2), 373–386, 1996.

Ilk, K. H.: Ein eitrag zur Dynamik ausgedehnter Körper-Gravitationswechselwirkung, Deutsche Geodätische Kommission. Reihe C, Heft Nr. 288, München, 1983.

Kotsiaros, S. and Olsen, N.: The geomagnetic field gradient tensor: Properties and parametrization in terms of spherical harmonics, Int. J. Geomath., 3, 297–314, 2012.

Kotsiaros, S. and Olsen, N.: End-to-End simulation study of a full magnetic gradiometry mission, Geophys. J. Int., 196(1), 100–110, 2014.

Kotsiaros, S., Finlay, C. C., and Olsen, N.: Use of along-track magnetic field differences in lithospheric field modelling, Geophys. J. Int., 200(2), 878–887, 2015.

Langel, R. A. and Hinze, W. J.: The Magnetic Field of the Earth’s Lithosphere: The Satellite Perspective, Cambridge University Press, Cambridge, United Kingdom, 1998.

Langlais, B., Lesur, V., Purucker, M. E., Connerney, J. E. P., and Mandea, M.: Crustal Magnetic Fields of Terrestrial Planets, Space Sci. Rev., 152, 223–249, 2010.

Lesur, V., Rother, M., Vervelidou, F., Hamoudi, M., and Thébault, E.: Post-processing scheme for modeling the lithsopheric magnetic field, Solid Earth, 4, 105–118, 2013.

Maus, S., Yin, F., Lühr, H., Manoj, C., Rother, M., Rauberg, J., Michaelis, I., Stolle, C., and Müller, R. D.: Resolution of direction of oceanic magnetic lineations by the sixth-generation lithospheric magnetic field model from CHAMP satellite magnetic measurements, Geochem. Geophys. Geosyst., 9(7), Q07021, doi:10.1029/2008GC001949, 2008.

Maus, S.: An ellipsoidal harmonic representation of Earth′s lithospheric magnetic field to degree and order 720, Geochem. Geophys. Geosyst., 11, Q06015, doi:10.1029/2010GC003026, 2010.

Olsen, N. and the Swarm End-to-End Consortium: Swarm-End-to-End mission performance simulator study, ESA contract No. 17263/02/NL/CB, DSRI Report 1/2004, Danish Space Research Institute, Copenhagen, 2004.

Olsen, N., Hulot, G., and Sabaka, T. J.: Sources of the Geomagnetic Field and the Modern Data That Enable Their Investigation, in: Handbook of Geomathematics, edited by: Freeden, W., Nashed, M. Z., and Sonar, T., Springer, Netherlands, 106–124, 2010.

Olsen, N., Lühr, H., Finlay, C. C., Sabaka, T. J., Michaelis, I., Rauberg, J., and Tøffner-Clausen, L.: The CHAOS-4 geomagnetic field model, Geophys. J. Int., 197: 815–827, 2014.

Olsen, N., Hulot, G., Lesur, V., Finlay, C. C., Beggan, C., Chulliat, A., Sabaka, T. J., Floberghagen, R., Friis-Christensen, E., Haagmans, R., Kotsiaros, S., Lühr, H, Tøffner-Clausen, L., and Vigneron, P.: The Swarm Initial Field Model for the 2014 geomagnetic field, Geophys. Res. Lett., 42, doi:10.1002/2014GL062659, 2015.

Pedersen, L. B. and Rasmussen, T. M.: The gradient tensor of potential field anomalies: Some implications on data collection and data processing of maps, Geophysics, 55(12), 1558–1566, 1990.

Petrovskaya, M. S. and Vershkov, A. N.: Non-singular expressions for the gravity gradients in the local north-oriented and orbital reference frames, J. Geod., 80, 117–127, 2006.

Purucker, M. E.: Lithospheric studies using gradients from close encounters of Ørsted, CHAMP and SAC-C, Earth Planets Space, 57, 1–7, 2005.

Purucker, M., Sabaka, T., Le, G., Slavin, J. A., Strangeway, R. J., and Busby, C.: Magnetic field gradients from the ST-5 constellation: Improving magnetic and thermal models of the lithosphere, Geophys. Res. Lett., 34, L24306, 2007.

Purucker, M. and Whaler, K.: Crustal magnetism, in: Treatise on Geophysics, vol. 5, Geomagnetism, edited by: Kono, M., Elsevier, Amsterdam, 195–237, 2007.

Ravat, D., Wang, B., Wildermuth, E., and Taylor, P. T.: Gradients in the interpretation of satellite-altitude magnetic data: an example from central Africa, J. Geodyn., 33, 131–142, 2002.

Ravat, D.: Interpretation of Mars southern highlands high amplitude magnetic field with total gradient and fractal source modeling: New insights into the magnetic mystery of Mars, Icarus, 214, 400–412, 2011.

Sabaka, T. J., Tøffner-Clausen, L., and Olsen, N.: Use of the Comprehensive Inversion method for Swarm satellite data analysis, Earth Planets Space, 65: 1201–1222, 2013.

Sabaka, T. J., Olsen, N., Tyler, R. H., and Kuvshinov, A.: CM5, a pre-Swarm comprehensive magnetic field model derived from over 12 years of CHAMP, Ørsted, SAC-C and observatory data, Geophys. J. Int., 200(3), 1596–1626, 2015.

Schmidt, P. and Clark, D.: Advantages of measuring the magnetic gradient tensor, Preview, 85, 26–30, 2000.

Schmidt, P. and Clark, D.: The magnetic gradient tensor: its properties and uses in source characterization, The Leading Edge, 25(1), 75–78, 2006.

Taylor, P. T., Kis, K. I., and Wittmann, G.: Satellite-altitude horizontal magnetic gradient anomalies used to define the Kursk magnetic anomaly, J. Appl. Geophys., doi:10.1016/j/jappgeo.2014.07.018, 2014.

Thébault, E., Purucker, M., Whaler, K. A., Langlais, B., and Sabaka, T. J.: The Magnetic Field of Earth's Lithosphere, Space Sci. Rev., 155, 95–127, 2010.

Wessel, P. and Smith, W. H. F.: Free software helps map and display data, EOS Trans. AGU, 72, 441&445–446, 1991.

403 **Tables and figures**

404

405 **Table 1.** Statistics of the magnetic potential, MV, MGT and third-order partial derivatives of the
406 magnetic potential field around the north pole ($0°\leq\theta\leq30°$) at the altitude of 300 km using the
407 lithospheric magnetic field model GRIMM_L120 (version 0.0) (Lesur et al., 2013) for spherical
408 harmonic degrees 16~90.

Magnetic effects	Minimum	Maximum	Mean	Standard deviation
V [mT×m]	-5.1554771	+4.7867519	+0.0828017	±1.7377648
B_x [nT]	-14.7389250	+17.6917740	-0.0890689	±4.9797007
B_y [nT]	-15.1297000	+13.6053000	+0.0010738	±4.8239313
B_z [nT]	-19.8715270	+25.3666030	-0.1988485	±6.7066701
B_{xx} [pT/m]	-0.1054684	+0.0621351	+0.0001872	±0.0215871
B_{xy} [pT/m]	-0.0410371	+0.0491030	+0.0000003	±0.0115018
B_{xz} [pT/m]	-0.0929498	+0.1082861	+0.0006867	±0.0247522
B_{yy} [pT/m]	-0.0726248	+0.0505990	-0.0004789	±0.0186580
B_{yz} [pT/m]	-0.0868184	+0.0826627	+0.0000058	±0.0228174
B_{zz} [pT/m]	-0.1015986	+0.1511038	+0.0002917	±0.0336965
$B_{xx}+B_{yy}+B_{zz}$ [pT/m]	-2.012×10^{-15}	$+2.026\times10^{-15}$	$+8.085\times10^{-19}$	$\pm5.101\times10^{-16}$
B_{xxz} [aT/m^2]	-0.7589853	+0.4794999	+0.0002436	±0.1537058
B_{xyz} [aT/m^2]	-0.2628265	+0.3734132	-0.0000004	±0.0734794
B_{xzz} [aT/m^2]	-0.7067652	+0.8470055	+0.0140820	±0.1752880
B_{yyz} [aT/m^2]	-0.5259662	+0.4076568	-0.0134321	±0.1370902
B_{yzz} [aT/m^2]	-0.6058631	+0.6396412	+0.0000341	±0.1448002
B_{zzz} [aT/m^2]	-0.7609268	+1.1697371	+0.0131885	±0.2421663

409

410 **Table 2.** Statistics of the magnetic potential, MV, MGT and third-order partial derivatives of the
411 magnetic potential field around the south pole ($150° \leq \theta \leq 180°$) at the altitude of 300 km using the
412 lithospheric magnetic field model GRIMM_L120 (version 0.0) (Lesur et al., 2013) for spherical
413 harmonic degrees 16~90.

Magnetic effects	Minimum	Maximum	Mean	Standard deviation
V [mT×m]	-3.3267455	+4.6543369	+0.0801853	±1.2427083
B_x [nT]	-11.440070	+15.9109730	+0.3451248	±3.5403285
B_y [nT]	-9.1169009	+15.0436160	-0.0001605	±3.1560093
B_z [nT]	-22.202857	+14.5020010	-0.3022955	±4.7971494
B_{xx} [pT/m]	-0.0579914	+0.0704617	+0.0000845	±0.0166266
B_{xy} [pT/m]	-0.0364002	+0.0308075	-0.0000006	±0.0074702
B_{xz} [pT/m]	-0.0741850	+0.0831062	+0.0019925	±0.0187492
B_{yy} [pT/m]	-0.0569493	+0.0706456	+0.0019055	±0.0143289
B_{yz} [pT/m]	-0.0599346	+0.0897167	-0.0000012	±0.0154623
B_{zz} [pT/m]	-0.1367168	+0.0735795	-0.0019900	±0.0258066
$B_{xx}+B_{yy}+B_{zz}$ [pT/m]	-1.027×10^{-15}	$+2.012\times10^{-15}$	$+1.113\times10^{-18}$	$\pm5.059\times10^{-16}$
B_{xxz} [aT/m^2]	-0.4605216	+0.5307263	+0.0011232	±0.1328515
B_{xyz} [aT/m^2]	-0.2840344	+0.2947601	-0.0000015	±0.0526629
B_{xzz} [aT/m^2]	-0.5686811	+0.5634376	0.0181792	±0.1497829
B_{yyz} [aT/m^2]	-0.4262850	+0.5819095	+0.0186968	±0.1169641
B_{yzz} [aT/m^2]	-0.6194116	+0.6520948	-0.0000118	±0.1085051
B_{zzz} [aT/m^2]	-1.0199774	+0.5863084	-0.0198200	±0.2084566

414

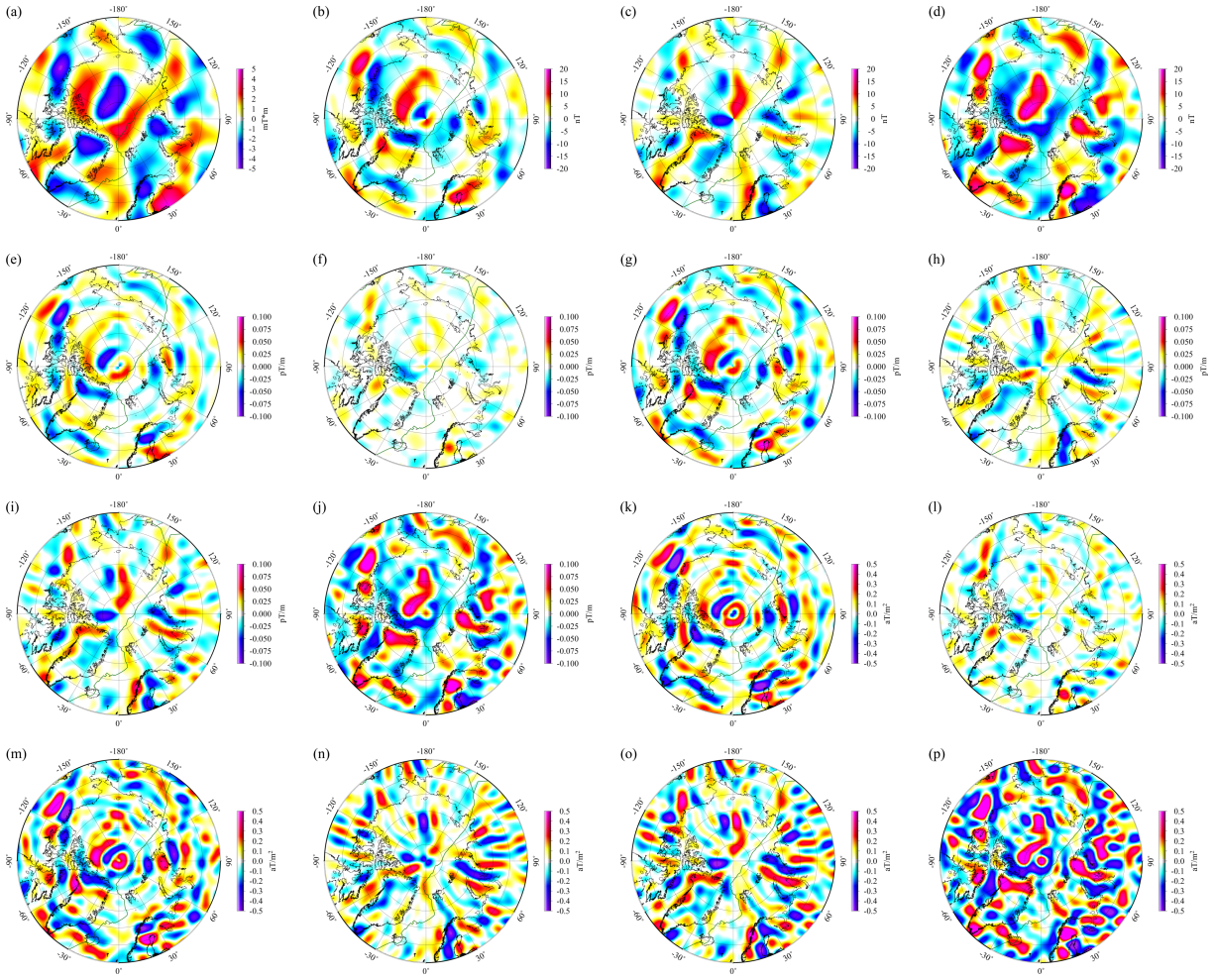

Figure 1. Lithospheric magnetic potential, vector and its gradients fields and third-order partial derivatives of the magnetic potential field around the north pole ($0°\leq\theta\leq30°$) at the altitude of 300 km as defined by the lithospheric magnetic field model GRIMM_L120 (version 0.0) (Lesur et al., 2013) for spherical harmonic degrees 16~90. (a) is magnetic potential (V), (b) (c) and (d) are three components (B_x, B_y and B_z) of magnetic vector, (e), (f), (g), (h), (i) and (j) are six elements (B_{xx}, B_{xy}, B_{xz}, B_{yy}, B_{yz} and B_{zz}) of magnetic gradient tensor, (k), (l), (m), (n), (o) and (p) are six elements (B_{xxz}, B_{xyz}, B_{xzz}, B_{yyz}, B_{yzz} and B_{zzz}) of third-order partial derivatives of the magnetic potential field, respectively. The dark green lines are the plate boundaries by Bird (2003). All maps are shown by Polar Stereographic projections.

415

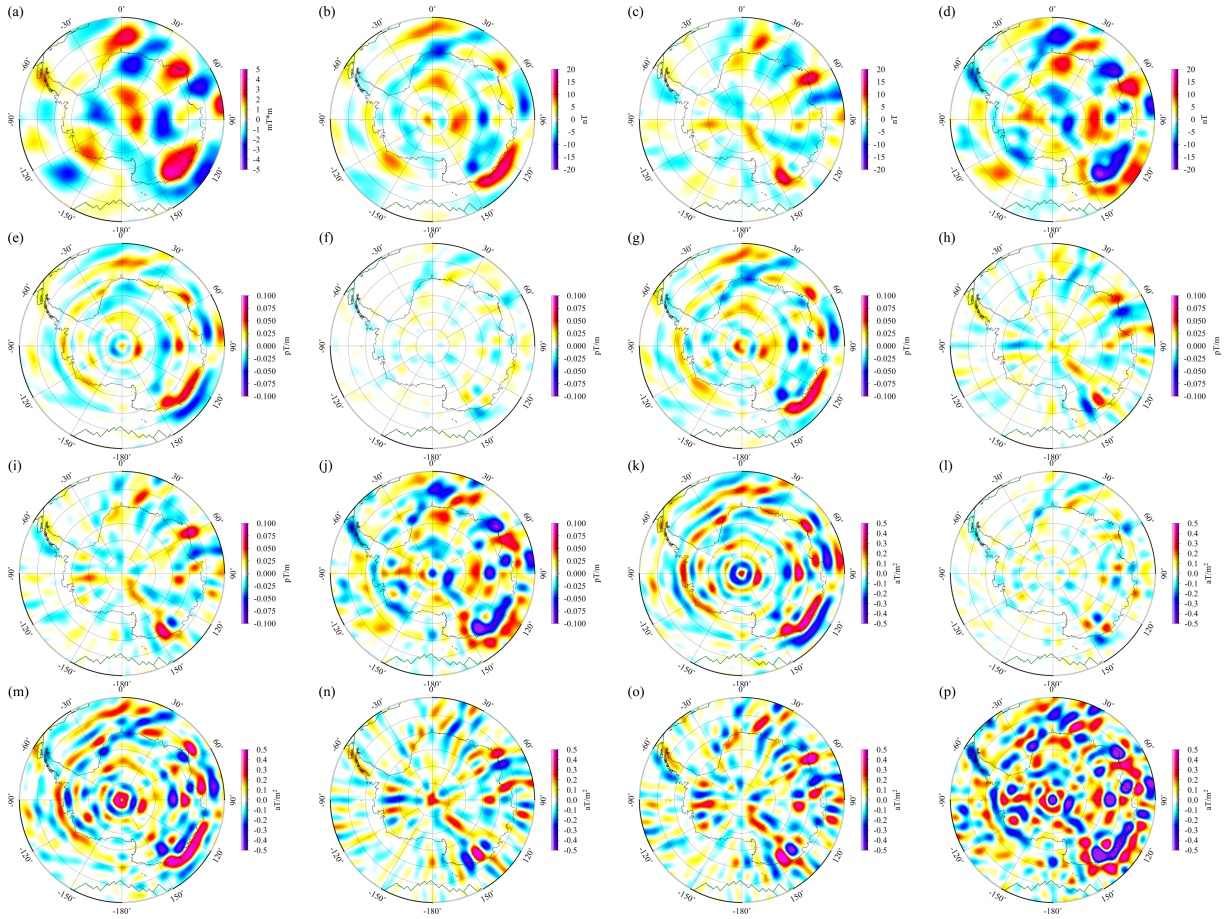

Figure 2. Lithospheric magnetic potential, vector and its gradients fields and third-order partial derivatives of the magnetic potential field around the south pole (150°≤θ≤180°) at the altitude of 300 km as defined by the lithospheric magnetic field model GRIMM_L120 (version 0.0) (Lesur et al., 2013) for spherical harmonic degrees 16~90. (a) is magnetic potential (V), (b) (c) and (d) are three components (B_x, B_y and B_z) of magnetic vector, (e), (f), (g), (h), (i) and (j) are six elements (B_{xx}, B_{xy}, B_{xz}, B_{yy}, B_{yz} and B_{zz}) of magnetic gradient tensor, (k), (l), (m), (n), (o) and (p) are six elements (B_{xxz}, B_{xyz}, B_{xzz}, B_{yyz}, B_{yzz} and B_{zzz}) of third-order partial derivatives of the magnetic potential field, respectively. The dark green lines are the plate boundaries by Bird (2003). All maps are shown by Polar Stereographic projections.

416

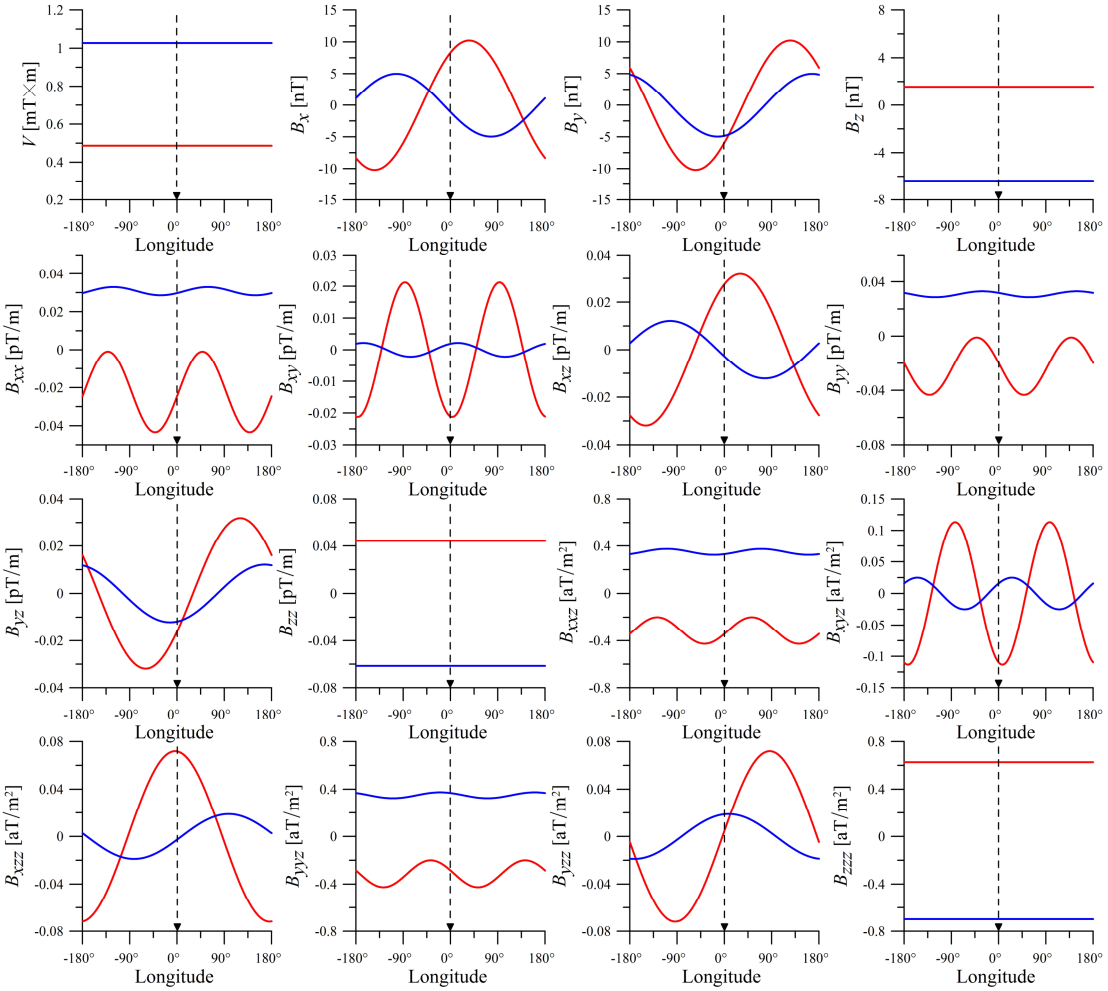

Figure 3. Limit values of magnetic potential (V), vector (B_x, B_y and B_z) and its gradients (B_{xx}, B_{xy}, B_{xz}, B_{yy}, B_{yz} and B_{zz}) and third-order partial derivatives of the magnetic potential field (B_{xxz}, B_{xyz}, B_{xzz}, B_{yyz}, B_{yzz} and B_{zzz}) at the poles when the local reference frames vary from different meridians (the direction of $\mathbf{x}_P$ axe changing from different meridian to the poles). Red and blue lines indicate the magnetic effects at north-pole and at south-pole, respectively. The reference frame is specially defined that the $\mathbf{x}_P$-axis points to the meridian of 180° E (or 180° W) at north pole and 0f 0° at south pole and the $\mathbf{y}_P$-axis points to the meridian of 90° E at two poles. The values at two poles showed by black dashed arrows are used to plot the maps in Fig. 1 and Fig. 2.

417